

MIT Open Access Articles

Path Selection in a Poisson field

The MIT Faculty has made this article openly available. **Please share** how this access benefits you. Your story matters.

Citation: Cohen, Yossi, and Daniel H. Rothman. "Path Selection in a Poisson Field." *Journal of Statistical Physics* 167.3–4 (2017): 703–712. © 2016 Springer Science+Business Media New York

As Published: <http://dx.doi.org/10.1007/s10955-016-1669-7>

Publisher: Springer-Verlag

Persistent URL: <http://hdl.handle.net/1721.1/109045>

Version: Author's final manuscript: final author's manuscript post peer review, without publisher's formatting or copy editing

Terms of use: Creative Commons Attribution-Noncommercial-Share Alike



Yossi Cohen · Daniel H. Rothman

Path selection in a Poisson field

Received: date / Accepted: date

Abstract A criterion for path selection for channels growing in a Poisson field is presented. We invoke a generalization of the principle of local symmetry. We then use this criterion to grow channels in a confined geometry. The channel trajectories reveal a self-similar shape as they reach steady state. Analyzing their paths, we identify a cause for branching that may result in a ramified structure in which the golden ratio appears.

1 Introduction

Pattern formation in Laplacian fields has been well-studied in recent decades [1–4]. Relevant models and processes include diffusion limited aggregation [5, 6], fracturing [3], dielectric breakdown [7] and viscous fingering [1, 2]. However, in spite of its broad relevance, many pattern formation processes, such as the generalized Stokes flow [8, 9], reaction-diffusion processes in chemical and biological systems [10], tearing of thin sheets [11, 12] and natural evolution of geological networks [13, 14], often involve Poisson dynamics, which changes the nature of the growth. While in the Laplacian case the forcing usually comes from the boundaries or from isolated sources inside the domain, in Poisson fields the driving force may be continuous throughout the domain. In these cases, much less theoretical work exists, even for the simple case of constant forcing, because the field becomes nonharmonic.

In a moving boundary problem, the motion of the boundary is typically dictated by the normal derivative of the field at each point on the boundary or the interface. However, in many cases, such as in a fracture in elastic materials [15, 16], river channels in a diffusion field [17], or flow patterns in a viscous fluid with zero surface tension [1, 2], the existence of a slit-like shape breaks the smoothness of the boundary and generates a singularity

Lorenz Center, Department of Earth Atmospheric, and Planetary Sciences, Massachusetts Institute of Technology, Cambridge, MA. 02139, USA

that attracts most of the flux into the tip (the point of singularity). Thus, the growth of a crack or a channel is much faster at its tip than at any other point along the boundary. Here we study the shape of the field in the neighborhood of a tip of a channel and derive predictions for path selection based on the Poisson flux entering the tip. Our objective here is to better understand the geometry of such *Poisson paths*.

To help fix ideas, consider the stream network in Figure 1. Groundwater, sourced by rainfall, flows diffusively to the streams, which can be taken to be absorbing boundaries. When the thickness of the groundwater layer is much smaller than its lateral extent, the Dupuit approximation [18–20] of hydrology yields the groundwater flow from the two-dimensional field ψ that solves the Poisson equation

$$\Delta\psi = -1, \quad (1)$$

where ψ is proportional to the square of the thickness of the groundwater layer and we have assumed constant rainfall and hydraulic conductivity. A model for network growth then follows if the following three ingredients can be derived from the Poisson field: the direction in which tips grow, the velocity at which they move, and the conditions that lead to bifurcation. Here, we primarily concern ourselves with the first and third ingredients.

We dedicate this paper to the memory of Leo P. Kadanoff. The related problem of Laplacian growth (wherein the right-hand side of equation (1) vanishes), especially as it manifests itself in two-dimensional viscous flow, occupied much of Leo’s attention (e.g., Ref. [21, 2]). Leo perceived such problems as opportunities for understanding the nature of physical law [22]: how simple mechanisms give rise to intricate structures such as the network of Figure 1, why such structures are ubiquitous in the natural world, and, perhaps most ambitiously, why these structures often seem to exemplify their own kind of simple physical laws. He also believed that a focus on “particular types of systems that really arise in the physical world” [22] constitutes a valuable approach toward these goals.

Accordingly, we note that casual inspection of Figure 1 suggests that streams branch at a characteristic angle and that tributaries of roughly equal length are spaced apart by roughly equal distances. The characteristic branching angle turns out to be $2\pi/5$ [23, 24]. Here, we suggest that the ratio of branch length to branch spacing is the golden ratio [25]. As we show below, these observations appear to derive from a particular way in which the trajectory of Poisson paths is similar to that taken by Laplacian paths [14]. If we are correct, we will have found a way in which a phenomenon conjectured to exist in the Laplace problem [26] exhibits itself in the seemingly more complicated Poisson problem.

The remainder of the paper is organized as follows. First, we show that paths taken in a Poisson field curve in such a way that preserves the symmetry of the field in the vicinity of channel tips. Next, we use this result to simulate the growth and interaction of growing channels. Two empirical observations emerge from simulations. First, there is a nearly constant spacing between paths at long times, independent of their initial positions. Second, there are universal features in the ways in which the curvature of the average path evolves. We show how these features can be related to the aforementioned

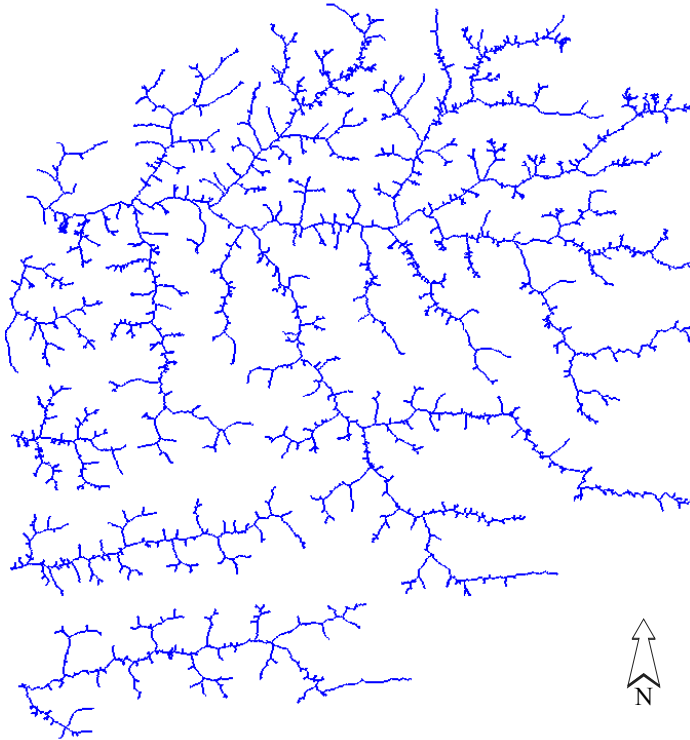


Fig. 1: A channel network located near Bristol FL [23]. The water flows toward the left.

characteristic angle of $2\pi/5$ [23,24] and the golden ratio. Finally, we discuss how these findings suggest a mechanism for branching.

2 The Laplacian case

A harmonic field (solution for the Laplace equation), at the vicinity of a tip of a slit (see Fig. 2), has the following shape when the field vanishes at the slit ($\Phi = 0$ for $\theta = \pm\pi$) [27,3],

$$\Phi(r, \theta) = a_1 r^{1/2} \cos\left(\frac{\theta}{2}\right) + a_2 r \sin(\theta) + \mathcal{O}(r^{3/2}). \quad (2)$$

where a_1, a_2 are coefficients defined by the global field and the boundary conditions, r is the distance from the tip and $\theta = 0$ points forward in the direction of the channel. The first term of the flux $-\nabla\phi$ has an inverse square-root singularity at the tip and its prefactor a_1 is usually called the intensity of the field [3]. Clearly, the first dominant term in Eq. (2) is symmetric with respect to the channel and therefore, the knowledge of the flux intensity alone

does not provide any other trajectory except from a straight path [3, 28, 29, 11]. To study path selection, we need to break the symmetry and consider also the asymmetric terms in the expansion.



Fig. 2: A semi-infinite channel.

In fracture mechanics, it is widely accepted that a crack evolves in a direction that maintains a symmetric field around it. For that, it was justified by showing that in this direction the crack releases the maximum elastic energy in its growth [3, 28, 27]. Since the first term in the expansion is symmetric with respect to the crack tip, it is necessary and sufficient to consider the next sub-dominant term that breaks the symmetry. Hence, the principle of local symmetry states that the evolution of the channel requires that this term goes to zero, i.e. a_2 must vanish. Path selection of a channel in a Laplacian field shares a similar property. It was recently shown that the growth of a channel according to the principle of local symmetry is equivalent to growth along the flow line intersecting with the channel tip [14, 30]. In this direction, the channel also maximizes locally the flux entering its tip. In the next section, we find the analog of the principle of local symmetry in a Poisson field for a constant forcing.

3 Local Symmetry and path selection in a Poisson field

The general Poisson equation in 2D can be expressed as

$$\Delta \Phi(x, y) = f(x, y), \quad (3)$$

where Φ is the Poisson field, $\Delta = (\frac{\partial^2}{\partial x^2} + \frac{\partial^2}{\partial y^2})$ is the Laplace operator and f , in general, can be any function. If $f = 0$, we have the Laplace equation, and Φ is an analytic function since it obeys Cauchy-Reimann conditions [31]. In this case, all the theorems of analytic functions in the complex plane can be used to find the field and to describe its properties. That is not the case when $f \neq 0$. In the Poisson equation, the field Φ is not an analytic function. However, in several cases when f is an analytic function and, in particular, a constant (a constant obeys Cauchy-Reimann conditions), $\Delta \Phi$ becomes an analytic function. For simplicity, we choose $f = -1$ and the Poisson equation as

$$\Delta \Phi = -1. \quad (4)$$

Applying the Laplace operator on both sides of Eq. (4), the field Φ becomes a solution of the bi-harmonic equation, i.e.

$$\Delta^2 \Phi = 0. \quad (5)$$

Although Φ is not an analytic function, we can express the field as the sum of two analytic functions [32],

$$\Phi(z, \bar{z}) = \Re\{\varphi(z)\bar{z} + \chi(z)\}. \quad (6)$$

where $\varphi(z)$ and $\chi(z)$ are unknown analytic functions, $z = x + iy$ is a complex number and \bar{z} is its complex conjugate. Applying Eq. (4) to Eq. (6),

$$\Delta \Phi \equiv 4\partial_z \partial_{\bar{z}} u = 4\Re\{\varphi'(z)\} = -1. \quad (7)$$

Since $\varphi(z)$ is an analytic function, its derivative $\varphi'(z)$ is also an analytic function. From Cauchy-Reimann equations, if a real part of an analytic function is identically constant, the function is a constant. Thus,

$$\varphi'(z) = C_1. \quad (8)$$

$C_1 = -\frac{1}{4} + iD_1$ and D_1 is a real number. Integrating once,

$$\varphi(z) = C_1 z + \overline{C_2}, \quad (9)$$

where $\overline{C_2}$ is an integration constant. Substituting $\varphi(z)$ in Eq. (6),

$$\Phi(z, \bar{z}) = \Re\{C_1 z \bar{z} + \overline{C_2} z + \chi(z)\}. \quad (10)$$

Note that $\Re\{\overline{C_2} z\} = \Re\{C_2 z\}$ and is analytic and thus can be included in the analytic function $\chi(z)$.

In the vicinity of the tip ($z = 0$) for a semi-infinite slit, the expansion of the analytic function $\chi(z)$ that satisfies the boundary condition $\Phi = 0$ at $\theta = \pm\pi$ becomes

$$\chi(z) = \frac{1}{4}z^2 + \sum_{n=1}^{\infty} i a_n (-z)^{\frac{n}{2}}, \quad n \in \mathbb{N}. \quad (11)$$

The coefficients a_n are real and are defined by the far field. Lastly, we can write the solution in polar coordinates,

$$\Phi(r, \theta) = \sum_{n=1,3,\dots} a_n r^{n/2} \cos(n\theta/2) + \sum_{n=2,4,\dots} a_n r^{n/2} \sin(n\theta/2) - \frac{1}{4}r^2(1 - \cos(2\theta)). \quad (12)$$

The expansion for the Poisson field around the slit in Fig. 2 is therefore similar to that for a Laplacian field up to the order of r^2 . The growth of a channel according to local symmetry considers only the first two dominant terms (up to the order of r), and therefore the requirement for a_2 holds as in Laplacian growth. In [14], it was shown empirically that this principle predicts the growth direction of streams in the river network shown in Fig. 1. We emphasize that although path selection and the growth mechanism are similar for both Laplacian and Poisson field, the trajectories are usually different because they are sensitive to the coefficients a_i that are determined by the global field.

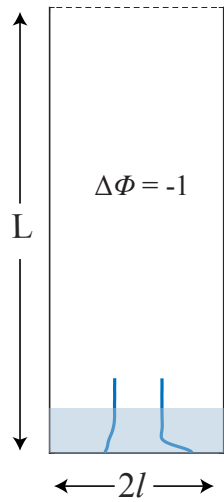


Fig. 3: The geometry of the domain. The boundary conditions are the following: Solid boundary and curves are absorbing ($\Phi = 0$); the dashed boundary is reflecting ($\frac{\partial\Phi}{\partial n} = 0$). The top boundary is far from the growing channels and was chosen as $L = 50l$. The marked area indicates the region that is magnified in Fig. 4.

4 Trajectories of growing channels

We now use this criterion for path selection to grow channels in a Poisson field in the geometry of Fig. 3. We initiate the channels at the bottom at random positions, perpendicular to the boundary $\{x = x_i; 0 < y < 0.01l\}$, where x_i was chosen randomly for the i -th channel out of a uniform distribution goes from $\{-0.8l, 0.8l\}$. The Poisson field $\Phi = 0$ along the channel. We allow the channels to grow with constant velocity according to the principle of local symmetry; we grow one channel in a small step each time in a different direction. Then we solve numerically the Poisson equation in the whole domain and study the first two terms in the expansion of the field, Eq. (12), in the vicinity of the channel. From the field, we find the coefficients of the expansion and choose the direction in which the second term in the expansion vanishes, i.e. gives $a_2 = 0$. More about this algorithm can be found in Appendix B of Ref. [14].

We start with two channels and grow them simultaneously according to the principle of local symmetry. In Fig. 4a, the trajectories of pairs of channel in 200 independent simulations are shown. Each channel initially curves and then converges toward a straight trajectory, results in dividing the box into three non-equal parts. The middle area between the two channels has almost a constant width of $l_c = 0.522 \pm 0.0007$, and two other areas bounded between one channel and the wall, with the average width of $l_w = 0.74 \pm 0.027$. The lengths l_c and l_w are normalized by half-width of the channel l . We also study the case of three channels in 150 simulations. As shown in Fig. 4b, we

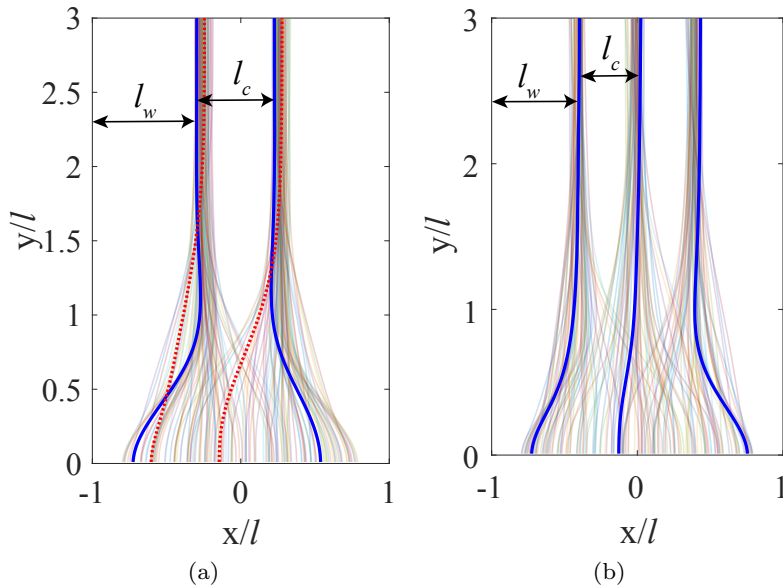


Fig. 4: The trajectories of channels in Poisson field. **(a.)** Simulations of two channels growing together. *Solid blue line*: an example of a pair initiated at opposite sides. *Dashed red line*: A pair of channels initiated in the left half of the domain. **(b.)** Simulations of three channels. *Solid blue line*: an example of a triplet in one simulation.

find that the channels again become closer to each other ($l_c = 0.39 \pm 0.013$) relative to the wall ($l_w = 0.60 \pm 0.031$). We note that evolving channels grow closer to each other than along a developed channel. This observation can be used to identify the growth order in a well-developed network.

5 Branching and the golden ratio

The above results address the motion and interaction of channel tips. We now address the conditions that lead channels to branch and form ramified structures such as the one shown in Figure 1. In fracture mechanics, a branching instability is usually associated with the splitting of a crack's tip when the crack propagation exceeds a critical velocity in a brittle material [33,34]. Here we suggest instead a side-branching mechanism. Although most of the Poisson flux goes to tips, it also goes to the sides of channels. As channels become more curved, the flux to the convex side increases while the flux to the concave side decreases. We conjecture that a new tip nucleates on the convex side of the most highly curved part of the trajectory. We proceed to consider geometric consequences of this conjecture.

Figure 5 shows that the average Poisson trajectory exhibits a clear maximum of the curvature. We denote the vertical coordinate of this maximum

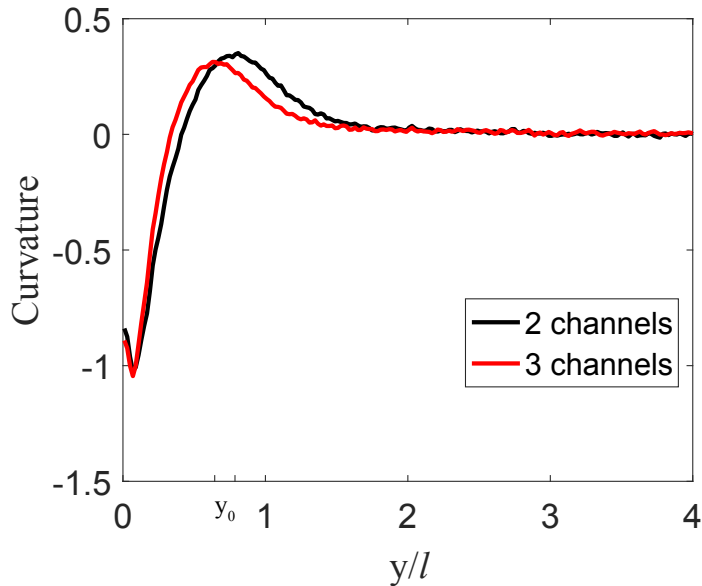


Fig. 5: The mean curvature as a function of y for simulations of two (black) and three (red) growing channels. A maximum is obtained at $y/l = y_0 = 0.81 \pm 0.02$ and $y_0 = 0.63 \pm 0.02$ for two and three channels, respectively. These results follow from averaging 200 two-trajectory simulations, and 150 simulations of three trajectories.

by y_0 , as shown in the schematic diagram of Figure 6. When two channels interact, we find that the average $y_0 = 0.81 \pm 0.02$. When three channels interact, the mean $y_0 = 0.63 \pm 0.02$. We expect that y_0 is analogous to a screening length, as it represents the (vertical) distance a path must travel beyond its origin (which is itself a kind of branch point). We also expect that l_c , the asymptotic distance between paths, should be related to y_0 . We find that $y_0/l_c = 1.56 \pm 0.05$ for the two-channel interaction and 1.61 ± 0.10 for the three-channel case. Both ratios are broadly consistent with the golden ratio $\phi = 1.618\dots$

Some years ago, Arneodo et al. [26] suggested that diffusion-limited aggregation—an archetypal model of Laplacian growth [6]—exhibits manifestations of the golden ratio and five-fold symmetry. Subsequent work has further shown how angles of $2\pi/5 = 72^\circ$ occur in other problems of Laplacian growth [35–37, 23, 24]. Angles of $2\pi/5$ and the golden ratio occur in the golden triangle, which contains two 72° angles and has sides of length 1 and ϕ [25]. Our Poisson paths do not grow in a Laplacian field, but as we showed earlier, aspects of their evolution are nevertheless similar. Do our Poisson trajectories exhibit angles of $2\pi/5$?

As discussed above, the interacting channels first move away from the nearest boundary or path, and later they are repelled by the nearest boundary

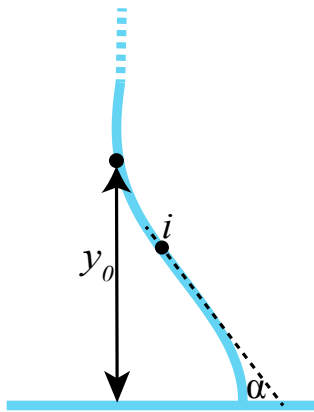


Fig. 6: An illustration of the channel shape. The curvature vanishes at the point of inflection i , and reaches maximum at a vertical distance y_0 from the bottom. The tangent at the point of inflection makes an angle α with respect to the horizontal.

or path on the other side. The point of transition corresponds to an inflection point in the trajectory where its curvature vanishes. We measure the angle α of the slope at the inflection, as indicated in Figure 6. The two-channel case yields $\alpha = 72.4^\circ \pm 10.3^\circ$; for the three-channel model, we find $74.7^\circ \pm 9.5^\circ$.

These results suggest that paths growing in a Poisson field exhibit some of the same geometric properties associated with Laplace systems. They also imply an interesting model of branching geometry. As shown schematically in Figure 7, “main” branches separated by a distance l_c give rise to secondary branches separated by a distance $y_0 = \phi l_c$, with branch points existing at locations with the highest curvature.

6 Discussion and Conclusion

Path selection in a Poisson field follows from an analogy with Laplacian growth: A channel develops in a direction that maintains locally a symmetric field around it. In this direction the sub-dominant term a_2 in the expansion of the field in the vicinity of the channel tip must vanish. Growing several channels in a Poisson field using this principle reveals three interesting phenomena: Constant spacing between channels, an apparent angle of 72° at the point of inflection, and a ratio of length scales that may equal the golden ratio.

Growing channels reach their steady state at a constant distance between each member and between the wall. A channel tends to move further from the absorbing wall, which can be regarded as an infinite channel, than to their neighboring growing channels. This interesting fact may be useful for analyzing the history of a network when some channels grow parallel to each other. The distance between the channels can indicate the growth order and the relative timing of when each channel evolves.

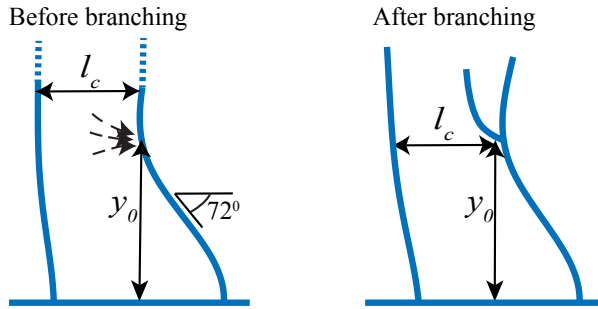


Fig. 7: Hypothesis for the geometry of the branching transition. Before branching, the point of highest curvature of the right-hand trajectory occurs at a normalized distance y_0 from the horizontal channel. At this point, the flux, which is the driving force for the growth and the evolution of the network, is maximized. This may cause nucleation of a new channel. The ratio $y_0/l_c = \phi$, the golden ratio. The slope of the trajectory at the point of inflection makes an angle of 72° with the horizontal.

We identify a length scale in which the channel reaches a maximum curvature that may cause a side-branching instability. This characteristic length, together with the angle of 72° at the point of inflection, generates an interesting structure that appears to culminate in the appearance of the golden ratio. Why this ratio prevails in a Poisson field is still not well understood.

7 Acknowledgement

We thank M. Z. Bazant, O. Devauchelle, M. Mineev-Weinstein and P. Szymczak for interesting discussions and helpful interactions. This work was supported by U.S. Department of Energy, Office of Science, Office of Basic Energy Sciences, Chemical Sciences, Geosciences, and Biosciences Division under Award Number FG02-99ER15004.

References

1. Philip Geoffrey Saffman and Geoffrey Taylor. The penetration of a fluid into a porous medium or hele-shaw cell containing a more viscous liquid. In *Proceedings of the Royal Society of London A: Mathematical, Physical and Engineering Sciences*, volume 245, pages 312–329. The Royal Society, 1958.
2. David Bensimon, Leo P Kadanoff, Shoudan Liang, Boris I Shraiman, and Chao Tang. Viscous flows in two dimensions. *Reviews of Modern Physics*, 58(4):977, 1986.
3. GI Barenblatt and G P Cherepanov. On brittle cracks under longitudinal shear. *Journal of Applied Mathematics and Mechanics*, 25(6):1654–1666, 1961.
4. David A Kessler, Joel Koplik, and Herbert Levine. Pattern selection in fingered growth phenomena. *Advances in Physics*, 37(3):255–339, 1988.
5. TA Witten Jr and Leonard M Sander. Diffusion-limited aggregation, a kinetic critical phenomenon. *Physical review letters*, 47(19):1400, 1981.

-
6. Thomas C Halsey. Diffusion-limited aggregation: a model for pattern formation. *Physics Today*, 53(11):36–41, 2000.
 7. L Niemeyer, L Pietronero, and HJ Wiesmann. Fractal dimension of dielectric breakdown. *Physical Review Letters*, 52(12):1033, 1984.
 8. Michael J Shelley, Fei-Ran Tian, and Krzysztof Wlodarski. Hele-shaw flow and pattern formation in a time-dependent gap. *Nonlinearity*, 10(6):1471, 1997.
 9. Robb McDonald and Mark Mineev-Weinstein. Poisson growth. *Analysis and Mathematical Physics*, 5(2):193–205, 2015.
 10. Martin Z Bazant. Exact solutions and physical analogies for unidirectional flows. *Physical Review Fluids*, 1(2):024001, 2016.
 11. Yossi Cohen and Itamar Procaccia. Dynamics of cracks in torn thin sheets. *Physical Review E*, 81(6):7, 2010.
 12. Yossi Cohen and Itamar Procaccia. Stress intensity factor of mode-III cracks in thin sheets. *Physical Review E*, 83(2):026106, 2011.
 13. Alexander P Petroff, Olivier Devauchelle, Arshad Kudrolli, and Daniel H Rothman. Four remarks on the growth of channel networks. *Comptes Rendus Geoscience*, 344(1):33–40, 2012.
 14. Yossi Cohen, Olivier Devauchelle, Hansjörg F Seybold, S Yi Robert, Piotr Szymczak, and Daniel H Rothman. Path selection in the growth of rivers. *Proceedings of the National Academy of Sciences*, 112(46):14132–14137, 2015.
 15. Alan A Griffith. The phenomena of rupture and flow in solids. *Philosophical transactions of the royal society of london. Series A, containing papers of a mathematical or physical character*, 221:163–198, 1921.
 16. GR Irwin. Analysis of stresses and strains near the end of a crack traversing a plate. *J. Appl. Mech.*, 1957.
 17. Thomas Dunne. Formation and controls of channel networks. *Progress in Physical Geography*, 4(2):211–239, 1980.
 18. J. Dupuit. *Études théoriques et pratiques sur le mouvement des eaux dans les canaux découverts et à travers les terrains perméables*. Dunod, 1863.
 19. J. Bear. *Dynamics of Fluids in Porous Media*. Dover Publications, New York, 1972.
 20. P. I. A. Polubarinova-Kochina. *Theory of Ground Water Movement*. Princeton University Press, Princeton, NJ, 1962.
 21. L. P. Kadanoff. Simulating hydrodynamics: a pedestrian model. *Journal of statistical physics*, 39(3-4):267–283, 1985.
 22. L. P. Kadanoff. On complexity. *Physics Today*, 40(3):7–9, 1987.
 23. O. Devauchelle, A. P. Petroff, H. F. Seybold, and D. H. Rothman. Ramification of stream networks. *Proceedings of the National Academy of Sciences*, 109(51):20832–20836, 2012.
 24. A. P. Petroff, O. Devauchelle, H. Seybold, and D. H. Rothman. Bifurcation dynamics of natural drainage networks. *Philosophical Transactions of the Royal Society A: Mathematical, Physical and Engineering Sciences*, 371(2004):20120365, 2013.
 25. M. Livio. *The Golden Ratio: The Story of Phi, the World’s Most Astonishing Number*. Random House LLC, 2008.
 26. A. Arneodo, F. Argoul, JF Muzy, and M. Tabard. Structural five-fold symmetry in the fractal morphology of diffusion-limited aggregates. *Physica A: Statistical Mechanics and its Applications*, 188(1-3):217–242, 1992.
 27. K Bertram Broberg. *Cracks and fracture*. Academic Press, 1999.
 28. R V Goldstein and R L Salganik. Brittle-fracture of solids with arbitrary cracks. *International Journal of Fracture*, 10(4):507–523, 1974.
 29. Vincent Hakim and Alain Karma. Laws of crack motion and phase-field models of fracture. *Journal of the Mechanics and Physics of Solids*, 57(2):342–368, 2009.
 30. Olivier Devauchelle and et al. Laplacian networks: growth, local symmetry and shape optimization. *TBD*, 2016.
 31. Milton Abramowitz and Irene A Stegun. *Handbook of mathematical functions: with formulas, graphs, and mathematical tables*, volume 55. Courier Corporation, 1964.

32. NI Muskhelishvili. *Some basic problems of the mathematical theory of elasticity*. Noordhoff, 1953.
33. E Katzav, M Adda-Bedia, and Rodrigo Arias. Theory of dynamic crack branching in brittle materials. *International Journal of Fracture*, 143(3):245–271, 2007.
34. Alain Karma and Alexander E Lobkovsky. Unsteady crack motion and branching in a phase-field model of brittle fracture. *Physical review letters*, 92(24):245510, 2004.
35. M. B. Hastings. Growth exponents with 3.99 walkers. *Physical Review E*, 64:046104, 2001.
36. L. Carleson and N. Makarov. Laplacian path models. *Journal d'Analyse Mathématique*, 87(1):103–150, 2002.
37. T. Gubiec and P. Szymczak. Fingered growth in channel geometry: A Loewner-equation approach. *Physical Review E*, 77(4):041602, Apr 2008.